

An Updated Study of B Meson Oscillations using Dilepton Events

The OPAL Collaboration

Abstract

This paper reports a study of B meson oscillations using hadronic Z^0 decays with two identified leptons, and updates a previous publication by including data collected in 1994. Decay times are reconstructed for each of the semileptonic B decays by forming vertices which include the lepton and by estimating the B meson momentum. The mass difference, Δm_d , between the two mass eigenstates in the B_d^0 system is measured to be $0.430 \pm 0.043 \begin{smallmatrix} +0.028 \\ -0.030 \end{smallmatrix} \text{ ps}^{-1}$, where the first error is statistical and the second error is systematic. For the B_s^0 system, a lower limit of $\Delta m_s > 2.2 \text{ ps}^{-1}$ is obtained at 95% C.L.

(To be submitted to Zeitschrift für Physik C)

The OPAL Collaboration

K. Ackerstaff⁸, G. Alexander²³, J. Allison¹⁶, N. Altekamp⁵, K.J. Anderson⁹, S. Anderson¹², S. Arcelli², S. Asai²⁴, D. Axen²⁹, G. Azuelos^{18,a}, A.H. Ball¹⁷, E. Barberio⁸, R.J. Barlow¹⁶, R. Bartoldus³, J.R. Batley⁵, S. Baumann³, J. Bechtluft¹⁴, C. Beeston¹⁶, T. Behnke⁸, A.N. Bell¹, K.W. Bell²⁰, G. Bella²³, S. Bentvelsen⁸, P. Berlich¹⁰, S. Bethke¹⁴, O. Biebel¹⁴, A. Biguzzi⁵, S.D. Bird¹⁶, V. Blobel²⁷, I.J. Bloodworth¹, J.E. Bloomer¹, M. Bobinski¹⁰, P. Bock¹¹, D. Bonacorsi², M. Boutemeur³⁴, B.T. Bouwens¹², S. Braibant¹², L. Brigliadori², R.M. Brown²⁰, H.J. Burckhart⁸, C. Burgard⁸, R. Bürgin¹⁰, P. Capiluppi², R.K. Carnegie⁶, A.A. Carter¹³, J.R. Carter⁵, C.Y. Chang¹⁷, D.G. Charlton^{1,b}, D. Chrisman⁴, P.E.L. Clarke¹⁵, I. Cohen²³, J.E. Conboy¹⁵, O.C. Cooke¹⁶, M. Cuffiani², S. Dado²², C. Dallapiccola¹⁷, G.M. Dallavalle², S. De Jong¹², L.A. del Pozo⁴, K. Desch³, M.S. Dixit⁷, E. do Couto e Silva¹², M. Doucet¹⁸, E. Duchovni²⁶, G. Duckeck³⁴, I.P. Duerdoth¹⁶, D. Eatough¹⁶, J.E.G. Edwards¹⁶, P.G. Estabrooks⁶, H.G. Evans⁹, M. Evans¹³, F. Fabbri², M. Fanti², A.A. Faust³⁰, F. Fiedler²⁷, M. Fierro², H.M. Fischer³, I. Fleck⁸, R. Folman²⁶, D.G. Fong¹⁷, M. Foucher¹⁷, H. Fukui²⁴, A. Fürstjes⁸, D.I. Futyan¹⁶, P. Gagnon⁷, J.W. Gary⁴, J. Gascon¹⁸, S.M. Gascon-Shotkin¹⁷, N.I. Geddes²⁰, C. Geich-Gimbel³, T. Gerasis²⁰, G. Giacomelli², P. Giacomelli⁴, R. Giacomelli², V. Gibson⁵, W.R. Gibson¹³, D.M. Gingrich^{30,a}, D. Glenzinski⁹, J. Goldberg²², M.J. Goodrick⁵, W. Gorn⁴, C. Grandi², E. Gross²⁶, J. Grunhaus²³, M. Gruwé⁸, C. Hajdu³², G.G. Hanson¹², M. Hansroul⁸, M. Hapke¹³, C.K. Hargrove⁷, P.A. Hart⁹, C. Hartmann³, M. Hauschild⁸, C.M. Hawkes⁵, R. Hawkings²⁷, R.J. Hemingway⁶, M. Herndon¹⁷, G. Herten¹⁰, R.D. Heuer⁸, M.D. Hildreth⁸, J.C. Hill⁵, S.J. Hillier¹, T. Hilse¹⁰, P.R. Hobson²⁵, R.J. Homer¹, A.K. Honma^{28,a}, D. Horváth^{32,c}, R. Howard²⁹, D.E. Hutchcroft⁵, P. Igo-Kemenes¹¹, D.C. Imrie²⁵, M.R. Ingram¹⁶, K. Ishii²⁴, A. Jawahery¹⁷, P.W. Jeffreys²⁰, H. Jeremie¹⁸, M. Jimack¹, A. Joly¹⁸, C.R. Jones⁵, G. Jones¹⁶, M. Jones⁶, U. Jost¹¹, P. Jovanovic¹, T.R. Junk⁸, D. Karlen⁶, V. Kartvelishvili¹⁶, K. Kawagoe²⁴, T. Kawamoto²⁴, R.K. Keeler²⁸, R.G. Kellogg¹⁷, B.W. Kennedy²⁰, J. Kirk²⁹, A. Klier²⁶, S. Kluth⁸, T. Kobayashi²⁴, M. Kobel¹⁰, D.S. Koetke⁶, T.P. Kokott³, M. Kolrep¹⁰, S. Komamiya²⁴, T. Kress¹¹, P. Krieger⁶, J. von Krogh¹¹, P. Kyberd¹³, G.D. Lafferty¹⁶, R. Lahmann¹⁷, W.P. Lai¹⁹, D. Lanske¹⁴, J. Lauber¹⁵, S.R. Lautenschlager³¹, J.G. Layter⁴, D. Lazic²², A.M. Lee³¹, E. Lefebvre¹⁸, D. Lellouch²⁶, J. Letts¹², L. Levinson²⁶, S.L. Lloyd¹³, F.K. Loebinger¹⁶, G.D. Long²⁸, M.J. Losty⁷, J. Ludwig¹⁰, A. Macchiolo², A. Macpherson³⁰, M. Mannelli⁸, S. Marcellini², C. Markus³, A.J. Martin¹³, J.P. Martin¹⁸, G. Martinez¹⁷, T. Mashimo²⁴, P. Mättig³, W.J. McDonald³⁰, J. McKenna²⁹, E.A. Mckigney¹⁵, T.J. McMahon¹, R.A. McPherson⁸, F. Meijers⁸, S. Menke³, F.S. Merritt⁹, H. Mes⁷, J. Meyer²⁷, A. Michelini², G. Mikenberg²⁶, D.J. Miller¹⁵, A. Mincer^{22,e}, R. Mir²⁶, W. Mohr¹⁰, A. Montanari², T. Mori²⁴, M. Morii²⁴, U. Müller³, K. Nagai²⁶, I. Nakamura²⁴, H.A. Neal⁸, B. Nellen³, R. Nisius⁸, S.W. O’Neale¹, F.G. Oakham⁷, F. Odorici², H.O. Ogren¹², N.J. Oldershaw¹⁶, M.J. Oreglia⁹, S. Orito²⁴, J. Pálincás^{33,d}, G. Pásztor³², J.R. Pater¹⁶, G.N. Patrick²⁰, J. Patt¹⁰, M.J. Pearce¹, S. Petzold²⁷, P. Pfeifenschneider¹⁴, J.E. Pilcher⁹, J. Pinfold³⁰, D.E. Plane⁸, P. Poffenberger²⁸, B. Poli², A. Posthaus³, H. Przysiezniak³⁰, D.L. Rees¹, D. Rigby¹, S. Robertson²⁸, S.A. Robins²², N. Rodning³⁰, J.M. Roney²⁸, A. Rooke¹⁵, E. Ros⁸, A.M. Rossi², M. Rosvick²⁸, P. Routenburg³⁰, Y. Rozen²², K. Runge¹⁰, O. Runolfsson⁸, U. Ruppel¹⁴, D.R. Rust¹², R. Rylko²⁵, K. Sachs¹⁰, T. Saeki²⁴, E.K.G. Sarkisyan²³, C. Sbarra²⁹, A.D. Schaile³⁴, O. Schaile³⁴, F. Scharf³, P. Scharff-Hansen⁸, P. Schenk³⁴, J. Schieck¹¹, P. Schleper¹¹, B. Schmitt⁸, S. Schmitt¹¹, A. Schöning⁸, M. Schröder⁸, H.C. Schultz-Coulon¹⁰, M. Schulz⁸, M. Schumacher³, C. Schwick⁸, W.G. Scott²⁰, T.G. Shears¹⁶, B.C. Shen⁴, C.H. Shepherd-Themistocleous⁸, P. Sherwood¹⁵, G.P. Sirolì², A. Sittler²⁷, A. Skillman¹⁵,

A. Skuja¹⁷, A.M. Smith⁸, G.A. Snow¹⁷, R. Sobie²⁸, S. Söldner-Rembold¹⁰, R.W. Springer³⁰,
M. Sproston²⁰, K. Stephens¹⁶, J. Steuerer²⁷, B. Stockhausen³, K. Stoll¹⁰, D. Strom¹⁹,
P. Szymanski²⁰, R. Tafirout¹⁸, S.D. Talbot¹, S. Tanaka²⁴, P. Taras¹⁸, S. Tarem²², R. Teuscher⁸,
M. Thiergen¹⁰, M.A. Thomson⁸, E. von Törne³, S. Towers⁶, I. Trigger¹⁸, E. Tsur²³, A.S. Turcot⁹,
M.F. Turner-Watson⁸, P. Utzat¹¹, R. Van Kooten¹², M. Verzocchi¹⁰, P. Vikas¹⁸, E.H. Vokurka¹⁶,
H. Voss³, F. Wäckerle¹⁰, A. Wagner²⁷, C.P. Ward⁵, D.R. Ward⁵, P.M. Watkins¹, A.T. Watson¹,
N.K. Watson¹, P.S. Wells⁸, N. Wermes³, J.S. White²⁸, B. Wilkens¹⁰, G.W. Wilson²⁷,
J.A. Wilson¹, G. Wolf²⁶, T.R. Wyatt¹⁶, S. Yamashita²⁴, G. Yekutieli²⁶, V. Zacek¹⁸, D. Zer-Zion⁸

¹School of Physics and Space Research, University of Birmingham, Birmingham B15 2TT, UK

²Dipartimento di Fisica dell' Università di Bologna and INFN, I-40126 Bologna, Italy

³Physikalisches Institut, Universität Bonn, D-53115 Bonn, Germany

⁴Department of Physics, University of California, Riverside CA 92521, USA

⁵Cavendish Laboratory, Cambridge CB3 0HE, UK

⁶ Ottawa-Carleton Institute for Physics, Department of Physics, Carleton University, Ottawa, Ontario K1S 5B6, Canada

⁷Centre for Research in Particle Physics, Carleton University, Ottawa, Ontario K1S 5B6, Canada

⁸CERN, European Organisation for Particle Physics, CH-1211 Geneva 23, Switzerland

⁹Enrico Fermi Institute and Department of Physics, University of Chicago, Chicago IL 60637, USA

¹⁰Fakultät für Physik, Albert Ludwigs Universität, D-79104 Freiburg, Germany

¹¹Physikalisches Institut, Universität Heidelberg, D-69120 Heidelberg, Germany

¹²Indiana University, Department of Physics, Swain Hall West 117, Bloomington IN 47405, USA

¹³Queen Mary and Westfield College, University of London, London E1 4NS, UK

¹⁴Technische Hochschule Aachen, III Physikalisches Institut, Sommerfeldstrasse 26-28, D-52056 Aachen, Germany

¹⁵University College London, London WC1E 6BT, UK

¹⁶Department of Physics, Schuster Laboratory, The University, Manchester M13 9PL, UK

¹⁷Department of Physics, University of Maryland, College Park, MD 20742, USA

¹⁸Laboratoire de Physique Nucléaire, Université de Montréal, Montréal, Quebec H3C 3J7, Canada

¹⁹University of Oregon, Department of Physics, Eugene OR 97403, USA

²⁰Rutherford Appleton Laboratory, Chilton, Didcot, Oxfordshire OX11 0QX, UK

²²Department of Physics, Technion-Israel Institute of Technology, Haifa 32000, Israel

²³Department of Physics and Astronomy, Tel Aviv University, Tel Aviv 69978, Israel

²⁴International Centre for Elementary Particle Physics and Department of Physics, University of Tokyo, Tokyo 113, and Kobe University, Kobe 657, Japan

²⁵Brunel University, Uxbridge, Middlesex UB8 3PH, UK

²⁶Particle Physics Department, Weizmann Institute of Science, Rehovot 76100, Israel

²⁷Universität Hamburg/DESY, II Institut für Experimental Physik, Notkestrasse 85, D-22607 Hamburg, Germany

²⁸University of Victoria, Department of Physics, P O Box 3055, Victoria BC V8W 3P6, Canada

²⁹University of British Columbia, Department of Physics, Vancouver BC V6T 1Z1, Canada

³⁰University of Alberta, Department of Physics, Edmonton AB T6G 2J1, Canada

³¹Duke University, Dept of Physics, Durham, NC 27708-0305, USA

³²Research Institute for Particle and Nuclear Physics, H-1525 Budapest, P O Box 49, Hungary

³³Institute of Nuclear Research, H-4001 Debrecen, P O Box 51, Hungary

³⁴Ludwigs-Maximilians-Universität München, Sektion Physik, Am Coulombwall 1, D-85748 Garching, Germany

^a and at TRIUMF, Vancouver, Canada V6T 2A3

^b and Royal Society University Research Fellow

^c and Institute of Nuclear Research, Debrecen, Hungary

^d and Department of Experimental Physics, Lajos Kossuth University, Debrecen, Hungary

^e and Depart of Physics, New York University, NY 1003, USA

1 Introduction

In the Standard Model, a second-order weak transition transforms neutral B mesons into their antiparticles [1]. The neutral B mesons therefore oscillate between particle and antiparticle states before decaying. The frequency of the oscillation depends on the top quark mass, the Cabibbo-Kobayashi-Maskawa matrix elements, and meson decay constants. By analogy with the K^0 case and neglecting CP violation, the mass eigenstates, $|B_1\rangle$ and $|B_2\rangle$, of B_q^0 ($q=d$ or s) can be described as follows:

$$\begin{aligned} |B_1\rangle &= \frac{1}{\sqrt{2}}(|B_q^0\rangle + |\bar{B}_q^0\rangle), \\ |B_2\rangle &= \frac{1}{\sqrt{2}}(|B_q^0\rangle - |\bar{B}_q^0\rangle). \end{aligned}$$

If a B_q^0 is produced at time $t = 0$, the probabilities of having a B_q^0 or a \bar{B}_q^0 at proper time t are¹

$$\begin{aligned} P_{B_q^0}(t) &= \frac{1}{\tau} e^{-t/\tau} \cos^2\left(\frac{\Delta m_q t}{2}\right) \\ P_{\bar{B}_q^0}(t) &= \frac{1}{\tau} e^{-t/\tau} \sin^2\left(\frac{\Delta m_q t}{2}\right) \end{aligned}$$

where τ is the B_q^0 lifetime. The frequency of the oscillation is given by Δm_q , the mass difference of the two mass eigenstates ($\Delta m_q = m_{B_1} - m_{B_2}$). For $B_d^0 - \bar{B}_d^0$ mixing, time-integrated measurements from ARGUS and CLEO give $x_d = \Delta m_d \tau = 0.67 \pm 0.08$ [2, 3]. Published measurements of the frequency of $B_d^0 - \bar{B}_d^0$ oscillations made at LEP are available using several different techniques [4, 5, 6, 7, 8]. Lower limits on Δm_s have been reported by the ALEPH [8, 9] and the OPAL [6, 7] collaborations.

Extracting information on CKM matrix elements from the measurements of Δm_d and Δm_s is prone to large uncertainties due to poorly known meson decay constants. These uncertainties can be reduced by considering the ratio $\Delta m_s/\Delta m_d$. Given the present knowledge of V_{ts} and V_{td} one expects Δm_s to be of the order of 10 ps^{-1} [10]. Using dilepton events in data collected between 1991 and 1993 [6], we studied $B_d^0 - \bar{B}_d^0$ and $B_s^0 - \bar{B}_s^0$ oscillations, reporting $\Delta m_d = 0.462^{+0.040}_{-0.053} {}^{+0.052}_{-0.035} \text{ ps}^{-1}$ and $\Delta m_s > 2.2 \text{ ps}^{-1}$ at 95% C.L. We update these results by including data collected in 1994. The technique is the same as that reported previously [6]. Hadronic Z^0 decays with two lepton candidates, one in each thrust hemisphere, are selected. The reconstruction of a secondary vertex that includes the lepton is attempted for each lepton candidate, yielding an estimate of the decay length of the b hadron. This is combined with an estimate of the relativistic boost of the b hadron to give the proper decay time. The likelihood of each event is calculated as a function of Δm_d and Δm_s according to the measured proper times and the charge combination of the two leptons. The result for Δm_d and the lower limit on Δm_s are then obtained using a maximum likelihood technique.

2 Event Selection and Simulation

¹The contribution of $\Delta\Gamma$, the difference between the total decay widths of the mass eigenstates, to the oscillations is expected to be negligible and has been ignored.

2.1 Event Selection

The analysis is performed on data collected by OPAL in the vicinity of the Z^0 peak from 1991 to 1994. The OPAL detector has been described elsewhere [11, 12]. Hadronic Z^0 decays are selected using criteria described in [13]. A cone jet algorithm [14] is used to classify tracks and electromagnetic clusters not associated to tracks into jets. The size of the cone is chosen so as to include nearly all the decay products of a b hadron into one jet. The jets also include particles produced in the fragmentation process, which originate from the e^+e^- collision point. A total of 2 874 660 hadronic events satisfy the event selection criteria.

Electrons are identified using an artificial neural network [6] which is trained on a sample of simulated hadronic Z^0 decays. Electrons from photon conversions are rejected as in [15]. Muons are identified as in [16]. Lepton candidates are required to satisfy $p > 2.0$ GeV and $|\cos\theta| < 0.9$. Additional kinematic criteria are imposed to reduce the fraction of leptons in the sample coming from cascade decays of the type $b \rightarrow c \rightarrow \ell$.

The techniques for secondary vertex reconstruction and proper time estimation are described in [6]. Dilepton events with at least one reconstructed vertex are selected.

2.2 Event Simulation

Monte Carlo events are used to predict the relative abundances and decay time distributions for lepton candidates from various physics processes. The JETSET 7.4 Monte Carlo program [17] with parameters tuned to OPAL data [18] is used to generate $Z^0 \rightarrow q\bar{q}$ events which are processed by the detector simulation program [19]. The fragmentation of b and c quarks is parametrised using the fragmentation function of Peterson *et al.* [20], with $\langle x_E \rangle$ for b and c hadrons given by the central values in Table 1.

Quantity	Value
$\langle x_E \rangle_b$	0.697 ± 0.013 [16]
$\langle x_E \rangle_c$	0.51 ± 0.02 [15]
$B(b \rightarrow \ell)$	$(10.5 \pm 0.6 \pm 0.5)\%$ [16]
$B(b \rightarrow c \rightarrow \ell)$	$(7.7 \pm 0.4 \pm 0.7)\%$ [16]
$B(b \rightarrow \bar{c} \rightarrow \ell)$	$(1.3 \pm 0.5)\%$ [16]
$M(B_s^0)$	5.48 GeV
$M(\Lambda_b)$	5.62 GeV
$\tau_{B^+}/\tau_{B_d^0}$	1.03 ± 0.06 [3]
$\tau_{B_s^0}/\tau_{B_d^0}$	1.03 ± 0.08 [3]
$\tau_{\Lambda_b}/\tau_{B_d^0}$	0.73 ± 0.06 [3]
$\langle \tau_b \rangle$	1.55 ± 0.02 ps [3]

Table 1: The parameters used for the Monte Carlo simulation.

Standard Model values of the partial widths of the Z^0 into $q\bar{q}$ are used [21]. The mixture of c-flavoured hadrons produced both in $Z^0 \rightarrow c\bar{c}$ events and in b hadron decays is as prescribed

in [15]. The semileptonic branching ratios of charm hadrons and associated uncertainties are also those of [15]. The central values in Table 1 are taken for the inclusive branching ratios for $b \rightarrow \ell$, $b \rightarrow c \rightarrow \ell$ and $b \rightarrow \bar{c} \rightarrow \ell$. The semileptonic branching ratios of the individual b hadrons are assumed to be proportional to the lifetimes. The models used in describing the semileptonic decays of b and c hadrons are those used in determining the central values in [15]. The assumed masses for B_s^0 and Λ_b particles are also given in Table 1. The lifetimes of b hadrons used in this analysis were taken from the world average values [3], as indicated in Table 1.

3 Fit Results for Δm_d

The numbers of dilepton events with at least one secondary vertex constructed for the combination of e-e, e- μ and μ - μ , are listed in Table 2, separately for like-sign and unlike-sign dilepton events. Also included is the total number of secondary vertices reconstructed in these events.

	e-e	e- μ	μ - μ	total	total vertices
unlike-sign	891	1791	1070	3752	5971
like-sign	377	780	448	1605	2573

Table 2: The numbers of dilepton events with at least one secondary vertex reconstructed for the combinations e-e, e- μ and μ - μ , separately for like-sign and unlike-sign leptons. Also indicated is the total number of secondary vertices reconstructed in unlike-sign and like-sign dilepton events.

In order to study Δm_d and Δm_s , the likelihood of the event sample is calculated as a function of these parameters. The construction of the likelihood function follows the procedure described in the previous paper [6]. The true proper time distribution is described by a physics function for each source of events. The B mixing is also described by the physics function. The reconstructed time distributions, $f(t)$, are then obtained by convolving the physics function with resolution functions, $P(t, t')$, which describe the proper time resolution for each source. For example, in the absence of mixing,

$$f(t) = \frac{1}{\tau} \int_0^\infty e^{-\frac{t'}{\tau}} P(t, t') dt'$$

for a source with lifetime τ . The resolution functions are complicated functions, which must include a description of misreconstruction near $t = 0$, even when the true proper time is large. The probability of this misreconstruction depends on the true proper time, and the description of the resolution function was modified from the previous paper to describe this better. The resolution function has the following form:

$$P(t, t') = C[(1 - \exp(-\frac{t'}{\alpha}))v(t, t') + \exp(-\frac{t'}{\alpha})u(t)]$$

where t and t' are the reconstructed proper time and the true proper time, respectively. The functions $v(t, t')$ and $u(t)$ describe the reconstructed proper time distributions for the correctly

reconstructed and misreconstructed vertices respectively. The parameter C is a normalization factor, while α is a parameter to describe the dependence of the misreconstruction probability on the true proper time. Distributions of t and $t - t'$ are shown in Figure 1 for three slices of true proper time t' for Monte Carlo b decays. The fitted resolution function, which is superimposed in the figure, describes the distributions well.

To determine Δm_d a three parameter fit is performed, varying Δm_d simultaneously with the cascade fraction, the fraction of lepton candidates in $Z \rightarrow b\bar{b}$ decays that are due to $b \rightarrow c \rightarrow \ell$ decays, and the B_s^0 production fraction, the fraction of b quarks that give rise to B_s^0 mesons. Gaussian constraints reflecting the systematic errors on these two parameters are imposed. The relative uncertainty in the cascade fraction is taken to be $\pm 15\%$ [15], which includes uncertainties due to branching fractions, decay modelling and detector simulation. The B_s^0 production fraction, f_s , is constrained both by direct measurements, giving a rate of $(11.1 \pm 2.6)\%$ [3] relative to all weakly decaying b hadrons, and by the measured average mixing rate of b hadrons, $\bar{\chi} = 0.126 \pm 0.008$ [3] together with knowledge of the equivalent parameters, χ_d and χ_s , for B_d^0 and B_s^0 mesons ($\chi_{d(s)} = 0.5 \times x_{d(s)}^2 / (1 + x_{d(s)}^2)$). This is equivalent to the constraint $f_s = (11.2_{-1.9}^{+1.8})\%$ [3] except that the values of χ_d and χ_s are calculated from the values of Δm_d and Δm_s in the fit, together with the appropriate lifetimes.

In the fit the B_s^0 oscillation parameter is fixed at $\Delta m_s = 10.0 \text{ ps}^{-1}$. The result of the fit is $\Delta m_d = 0.430 \pm 0.045 \text{ ps}^{-1}$. The fitted value of the cascade fraction is 0.078 ± 0.007 compared to the nominal value of 0.066, as calculated from the Monte Carlo sample. The fitted value of f_s is $(12.7 \pm 1.9)\%$.

Figure 2 shows the distribution of decay times for all leptons in the dilepton sample and separately for leptons in like-sign and unlike-sign events. The curves are the results of the likelihood fit.

The fraction of like-sign leptons as a function of proper decay time,

$$\mathcal{R}(t) = \frac{N^{LS}(t)}{N^{US}(t) + N^{LS}(t)},$$

is plotted in Figure 3 for data, where $N^{LS}(t)$ ($N^{US}(t)$) is the reconstructed time distribution for leptons in like-sign (unlike-sign) events. In the figure, the expected curve for $\Delta m_d = 0.430 \text{ ps}^{-1}$ is shown as the solid line. The fitted values of the cascade fraction and the fraction of leptons from B_s^0 decays are used. Events in which vertices have been reconstructed in both thrust hemispheres enter the plot twice.

4 Systematic Errors on Δm_d

In the three parameter fit, the error on Δm_d is a combination of statistical error and systematic error due to the constraints on the cascade decay fraction and the B_s^0 production fraction. The systematic error from the cascade decay fraction is estimated by repeating the fit with the central value of the constraint for the cascade fraction changed by $+15\%$ or -15% (the systematic uncertainty on this parameter) from its nominal value. The systematic error resulting from the B_s^0 production fraction is obtained in a similar way. The statistical error on Δm_d is

$\pm 0.043 \text{ ps}^{-1}$, obtained by subtracting in quadrature these two systematic errors from the fit error.

The uncertainty due to the resolution function description is assessed by repeating the parametrisation using Monte Carlo events in which the tracking resolution is degraded by 10% [22] or improved by 10%. The uncertainty in the background from $Z^0 \rightarrow c\bar{c}$ events is taken to be $\pm 30\%$ due to uncertainties in the branching fractions and modelling of semileptonic charm decays, the relative production rates of charmed hadrons, and the uncertainty in the partial width for $Z^0 \rightarrow c\bar{c}$. The production rates of B_d^0 and B^+ are assumed to be equal and the b-baryon production rate is assumed to lie in the range $(9 \pm 4)\%$. The fraction of D^{**} produced in decays of b hadrons was assumed to be $B(b \rightarrow D^{**}) = 0.36 \pm 0.10$. Variations in the efficiency of the secondary vertex reconstruction as a function of decay length are found to have a negligible effect on Δm_d . Uncertainties in the source composition due to Monte Carlo statistics are negligible. The B lifetime variations are performed by changing the ratios of individual B lifetimes while keeping the average lifetime fixed at the LEP, CDF and SLD average value, 1.55 ps^{-1} .

The summary of the sources and estimated values of systematic errors is given in Table 3. The sum of these systematic errors in quadrature is $\delta\Delta m_d = {}^{+0.028}_{-0.030} \text{ ps}^{-1}$.

Source of uncertainty and range	$\delta\Delta m_d \text{ ps}^{-1}$
cascade decay fraction ($\pm 15\%$)	-0.010 +0.011
B_s^0 fraction (see text)	-0.006 +0.006
resolution function ($\pm 10\%$)	+0.010 -0.010
lepton misidentification (e: $\pm 30\%$, μ : $\pm 20\%$)	-0.001 +0.000
charm background ($\pm 30\%$)	-0.006 +0.001
b-baryon fraction (± 0.04)	+0.010 -0.009
$B(b \rightarrow D^{**})$ (± 0.10)	+0.003 -0.003
$\tau_{B^+}/\tau_{B_d^0} = 1.03 \pm 0.06$	+0.019 -0.023
$\tau_{B_s^0}/\tau_{B_d^0} = 1.03 \pm 0.08$	-0.000 +0.001
$\tau_{\Lambda_b}/\tau_{B_d^0} = 0.73 \pm 0.06$	+0.004 -0.004
$\Delta m_s = 2 - 20 \text{ ps}^{-1}$	+0.004 -0.000
Total systematic error	+0.028 -0.030

Table 3: Summary of systematic errors on the Δm_d measurement. For each source of error, the first error quoted results from varying the parameter in the positive sense.

5 Fit Results for Δm_s

We use the dependence of the likelihood on the assumed value of Δm_s to derive a lower limit. To account for systematic errors when setting the limit, we produce a likelihood curve as a function of Δm_s that includes these effects. This is achieved by maximizing the likelihood with respect to the value of each relevant parameter, constrained by a Gaussian error corresponding to its uncertainty, at each value of Δm_s . The constraints are those shown in Table 3. In addition, Δm_d is treated as a systematic uncertainty constrained by the average Δm_d from

analyses using reconstructed D^* mesons: $\Delta m_d = 0.52 \pm 0.05 \text{ ps}^{-1}$ [4, 5]. The exception to this scheme is the treatment of the resolution function description. In this case, three curves of $\ln \mathcal{L}$ were calculated, including all other systematic uncertainties, assuming the default tracking resolution or assuming the tracking resolution was degraded or improved by 10%. The smallest of the three values of $-\Delta \ln \mathcal{L}$ was taken at each value of Δm_s . The solid curve in Figure 4 shows the difference in log-likelihood from the maximum as a function of Δm_s with systematic errors included.

We set the limit on the basis of the difference in log-likelihood, $\Delta \ln \mathcal{L}$, with respect to the maximum value. A Monte Carlo technique was used to determine the correspondence between confidence levels and values of $\Delta \ln \mathcal{L}$ as a function of Δm_s . This approach is found to be more reliable than the approach of the previous paper [6], where $-\Delta \ln \mathcal{L} = 1.92$ was assumed to correspond to 95% confidence level. Many data sets, of the same size as the real data sample, were simulated using a fast Monte Carlo and fitted in a manner similar to the data. The main systematic errors affecting the Δm_s result were simulated by allowing the parameters of the Monte Carlo to vary independently for each data set. The corresponding parameters were allowed to vary under Gaussian constraints in the fit. The exception to this was the parameter governing the proper time resolution, which was treated in the same way as in the data fit. For each simulated data sample a single value of $\Delta \ln \mathcal{L} = \ln \mathcal{L}_{\max} - \ln \mathcal{L}(\Delta m_s^*)$ was extracted, where Δm_s^* is the generated value of Δm_s . The $\Delta \ln \mathcal{L}$ corresponding to 95% confidence was defined to be that value above which lay only 5% of the simulated data samples. This procedure was performed for input values of $\Delta m_s^* = 1.0, 2.0, 4.0$ and 8.0 ps^{-1} , using 3000 Monte Carlo data sets at each value of Δm_s^* . The results of this study are shown as the dashed line in Figure 4. We exclude the region of $\Delta m_s < 2.2 \text{ ps}^{-1}$ at 95% C.L.

To assess the importance of the systematic errors, we studied the log-likelihood as a function of Δm_s , while fixing all other parameters. These parameters were set to the values that maximized the log-likelihood at the preferred value of Δm_s in the procedure described above. The result is shown as the dotted curve in Figure 4. We conclude that the systematic errors have only a minor effect on our result.

Using the data sets simulated with the fast Monte Carlo referred to above, we were able to check the analysis technique and study the expected sensitivity to Δm_s . The results of these studies are shown in Figure 5. Each row corresponds to a different generated value of Δm_s , indicated by the Δm_s^* at the right edge of the plot. The left column shows the fitted value of Δm_s for each trial. In the right column are normalised cumulative distributions of the log-likelihood difference between the value at the fitted maximum and the value at the generated Δm_s for each trial. The sensitivity of this analysis is good for $\Delta m_s^* < 4 \text{ ps}^{-1}$, but is lost between 4 ps^{-1} and 8 ps^{-1} .

6 Conclusion

We have measured the oscillation frequency Δm_d by measuring the proper time of B meson decays and tagging the charges of leptons in both thrust hemispheres. The $B_d^0 - \bar{B}_d^0$ oscillation parameter is measured to be:

$$\Delta m_d = 0.430 \pm 0.043 \begin{matrix} +0.028 \\ -0.030 \end{matrix} \text{ ps}^{-1} ,$$

corresponding to $(2.83 \pm 0.28_{-0.20}^{+0.18}) \times 10^{-4}$ eV. This result is consistent with and supersedes the result using 1991-1993 data.

The Δm_d value is consistent with the OPAL results $\Delta m_d = 0.548 \pm 0.050_{-0.019}^{+0.023}$ ps⁻¹ [5] from data containing D^{*±} mesons and leptons, and $\Delta m_d = 0.444 \pm 0.029_{-0.017}^{+0.020}$ ps⁻¹ [7] from inclusive lepton events. Combining these results, taking into account correlations in the systematic errors, we find

$$\Delta m_d = 0.467 \pm 0.022_{-0.015}^{+0.017} \text{ ps}^{-1} .$$

The small statistical correlations between the results were found to have a negligible effect. This result is consistent with previous measurements [4, 8]. Using $\tau_{B_d^0} = 1.56 \pm 0.06$ ps, the combined OPAL value gives $x_d = 0.73 \pm 0.04 \pm 0.03$, where the last error is due to the uncertainty in $\tau_{B_d^0}$. This value is also consistent with the average of ARGUS and CLEO measurements, $x_d = 0.67 \pm 0.08$ [2, 3].

We obtain a lower limit on Δm_s at 95% confidence level: $\Delta m_s > 2.2$ ps⁻¹. This limit is less constraining than the ALEPH results[8, 9] and a recent OPAL result [7].

Acknowledgements

We particularly wish to thank the SL Division for the efficient operation of the LEP accelerator and for their continuing close cooperation with our experimental group. We thank our colleagues from CEA, DAPNIA/SPP, CE-Saclay for their efforts over the years on the time-of-flight and trigger systems which we continue to use. In addition to the support staff at our own institutions we are pleased to acknowledge the

Department of Energy, USA,

National Science Foundation, USA,

Particle Physics and Astronomy Research Council, UK,

Natural Sciences and Engineering Research Council, Canada,

Israel Science Foundation, administered by the Israel Academy of Science and Humanities,

Minerva Gesellschaft,

Benozio Center for High Energy Physics,

Japanese Ministry of Education, Science and Culture (the Monbusho) and a grant under the Monbusho International Science Research Program,

German Israeli Bi-national Science Foundation (GIF),

Direction des Sciences de la Matière du Commissariat à l'Énergie Atomique, France,

Bundesministerium für Bildung, Wissenschaft, Forschung und Technologie, Germany,

National Research Council of Canada,

Hungarian Foundation for Scientific Research, OTKA T-016660, T023793 and OTKA F-023259.

References

- [1] See for example: P. Franzini, *Physics Reports* **173** (1989) 1.
- [2] ARGUS Collaboration, H. Albrecht *et al.*, *Z. Phys.* **C 55** (1992) 357;
ARGUS Collaboration, H. Albrecht *et al.*, *Phys. Lett.* **B 324** (1994) 249;
CLEO Collaboration, J. Bartelt *et al.*, *Phys. Rev. Lett.* **71** (1993) 1680.
- [3] Particle Data Group, ‘Review of Particle Physics’, *Phys. Rev.* **D 54** (1996) 1.
- [4] ALEPH Collaboration, D. Buskulic *et al.*, *Phys. Lett.* **B 313** (1993) 498;
DELPHI Collaboration, P. Abreu *et al.*, *Phys. Lett.* **B 338** (1994) 409;
DELPHI Collaboration, P. Abreu *et al.*, *Z. Phys.* **C 72** (1996) 17;
L3 Collaboration, M. Acciarri *et al.*, *Phys. Lett.* **B 383** (1996) 487;
ALEPH Collaboration, D. Buskulic *et al.*, CERN-PPE/96-102, submitted to *Z. Phys. C*.
- [5] OPAL Collaboration, G. Alexander *et al.*, *Z. Phys.* **C 72** (1996) 377.
- [6] OPAL Collaboration, R. Akers *et al.*, *Z. Phys.* **C 66** (1995) 555.
- [7] OPAL Collaboration, K. Ackerstaff *et al.*, CERN-PPE/97-36, submitted to *Z. Phys. C*.
- [8] ALEPH Collaboration, D. Buskulic *et al.*, *Phys. Lett.* **B 322** (1994) 441.
- [9] ALEPH Collaboration, D. Buskulic *et al.*, *Phys. Lett.* **B 356** (1995) 409;
ALEPH Collaboration, D. Buskulic *et al.*, *Phys. Lett.* **B 377** (1996) 205.
- [10] Y. Nir, *Phys. Lett.* **B 327** (1994) 85;
A. Ali and D. London, *Z. Phys.* **C 65** (1995) 431.
- [11] OPAL Collaboration, K. Ahmet *et al.*, *Nucl. Inst. and Meth.* **A 305** (1991) 275.
- [12] P. Allport *et al.*, *Nucl. Inst. and Meth.* **A 324** (1993) 34;
P. Allport *et al.*, *Nucl. Inst. and Meth.* **A 346** (1994) 476.
- [13] OPAL Collaboration, G. Alexander *et al.*, *Z. Phys.* **C 52** (1991) 175.
- [14] OPAL Collaboration, R. Akers *et al.*, *Z. Phys.* **C 63** (1994) 197.
The jet finding parameters ϵ and R are set to 5.0 GeV and 0.65, respectively.
- [15] OPAL Collaboration, P. Acton *et al.*, *Z. Phys.* **C 58** (1993) 523.
- [16] OPAL Collaboration, R. Akers *et al.*, *Z. Phys.* **C 60** (1993) 199.
- [17] T. Sjöstrand, *Comp. Phys. Comm.* **82** (1994) 74.
- [18] OPAL Collaboration, G. Alexander *et al.*, *Z. Phys.* **C 69** (1996) 543.
- [19] J. Allison *et al.*, *Nucl. Instrum. Methods* **A 317** (1992) 47.
- [20] C. Peterson, D. Schlatter, I. Schmitt and P. Zerwas, *Phys. Rev.* **D 27** (1983) 105.

- [21] D. Bardin *et al.*, *ZFITTER, An Analytical Program for Fermion Pair Production in e^+e^- Annihilation*, CERN-TH/6443-92.
For this prediction, the Z^0 , top quark, and Higgs boson masses are set to $M_{Z^0} = 91.18$ GeV, $M_{\text{top}} = 150$ GeV and $M_{\text{Higgs}} = 300$ GeV, and $\alpha_s = 0.12$.
- [22] OPAL Collaboration, R. Akers *et al.*, *Z. Phys. C* **65** (1995) 17.

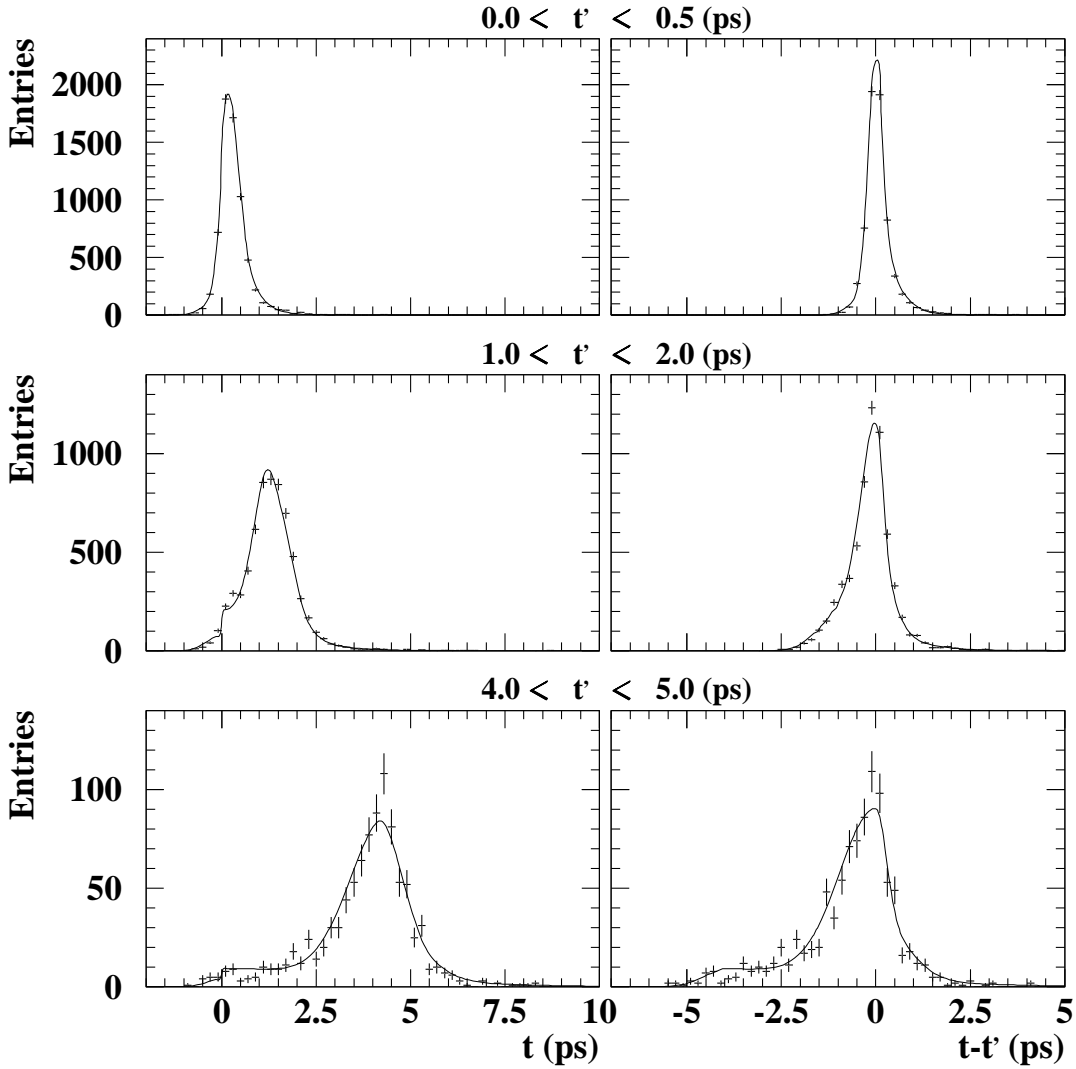


Figure 1: The distributions of reconstructed proper time, t , and $t - t'$ in three slices of the true proper time t' for leptons from primary b hadron decays in the Monte Carlo. Also shown is the parametrisation of these distributions.

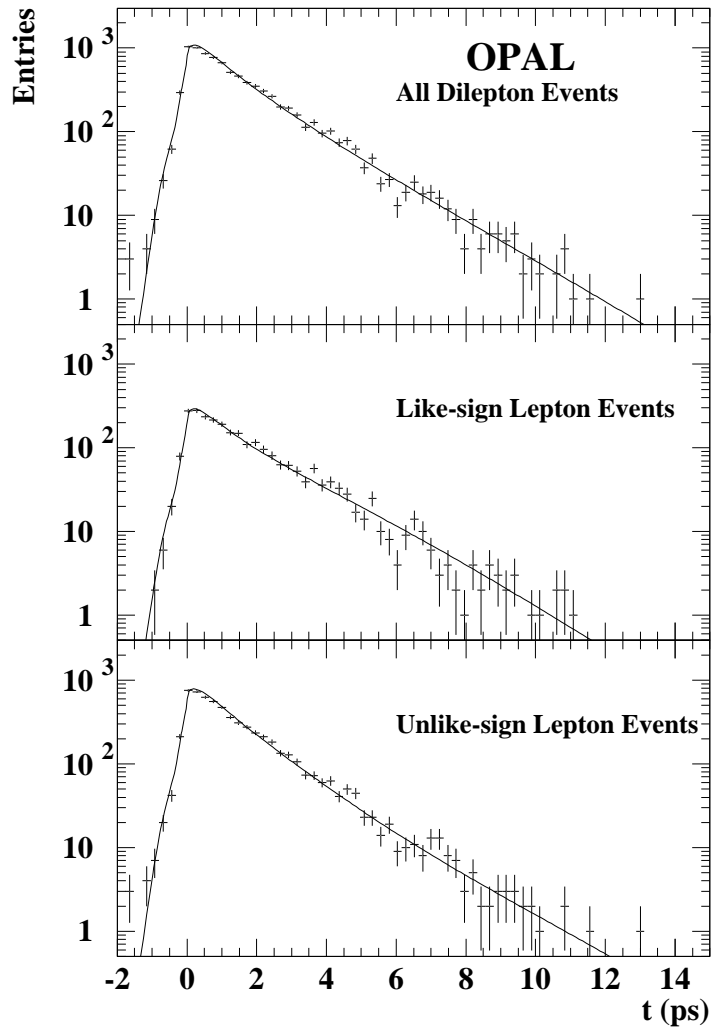


Figure 2: The proper time distributions for all leptons in dilepton events (top) for which a vertex is found, and for those leptons in like-sign (centre) and unlike-sign (bottom) events. The curves represent the results of the maximum likelihood fit.

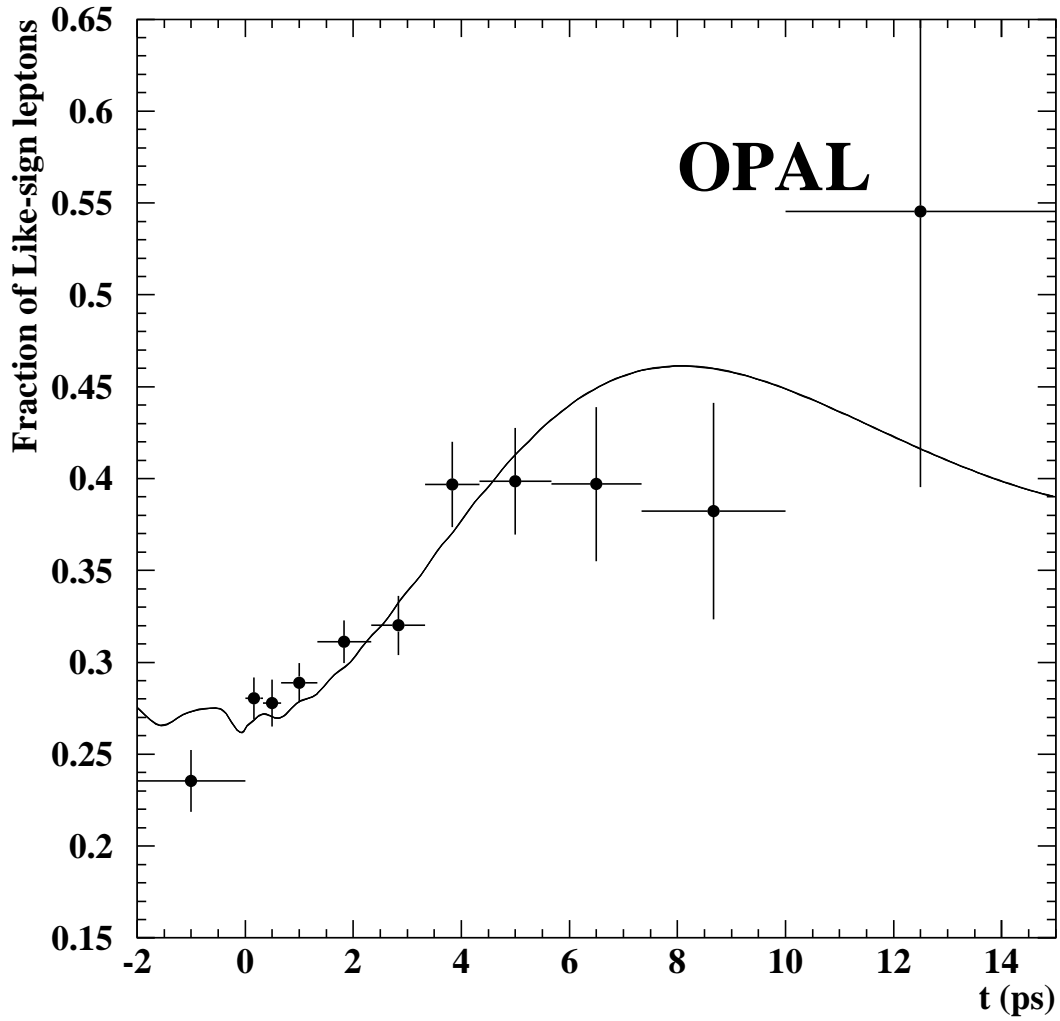


Figure 3: The fraction of like-sign leptons as a function of proper decay time: $\mathcal{R}(t)$. The solid curve represents the expectation with Δm_d set to 0.430 ps^{-1} and Δm_s set to 10.0 ps^{-1} .

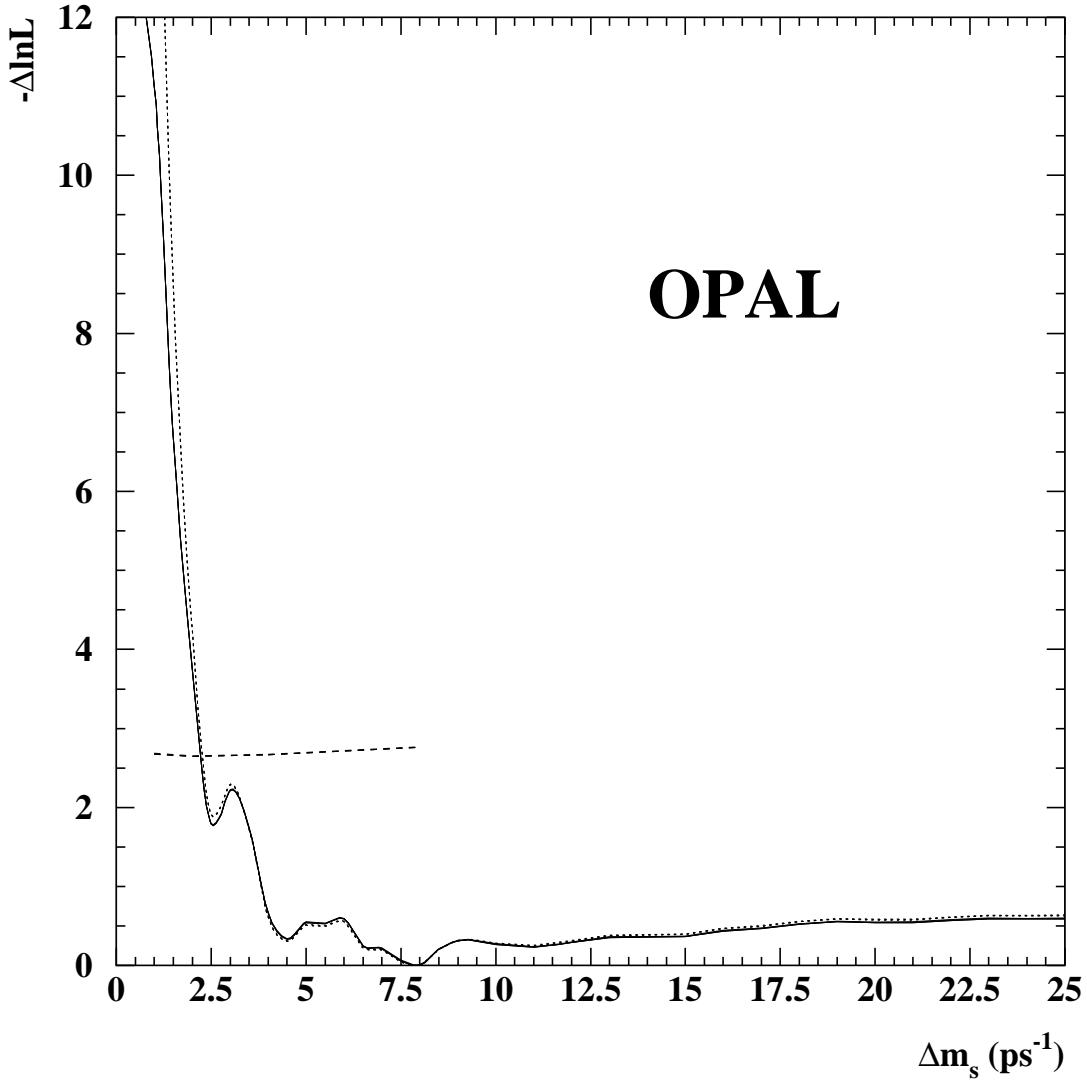


Figure 4: The difference in log-likelihood from the maximum value is shown as a function of Δm_s . The solid curve includes the effect of systematic errors, while the dotted curve includes only statistical errors. The dashed curve shows the 95% C.L.

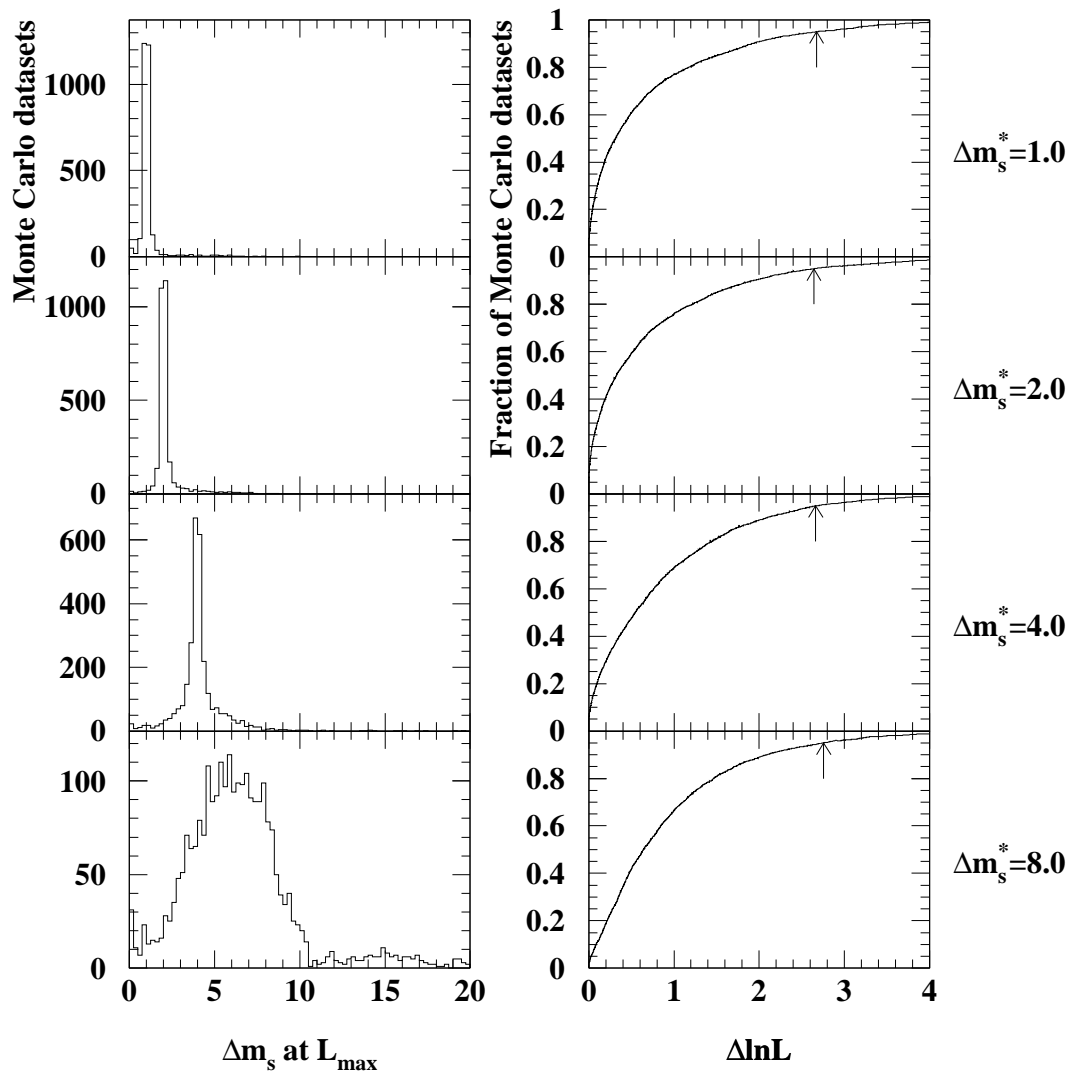


Figure 5: The results of fits to 3000 toy Monte Carlo datasets are shown. The Δm_s^* value indicates the generated value of Δm_s in ps^{-1} . The left-hand column shows the distribution of fitted values of Δm_s for each Δm_s^* value. The right-hand column shows the normalised cumulative distribution of the difference between the log-likelihood values at the fitted maximum and at the generated value. The arrow indicates the 95% confidence level value.